THE JOURNAL OF PHYSICAL CHEMISTRY B

ARTICLE

pubs.acs.org/JPCB

Orientation of α-Sexithiophene on Friction-Transferred Polythiophene Film

Toshiko Mizokuro,* Claire Heck, and Nobutaka Tanigaki

Research Institute for Ubiquitous Energy Devices, National Institute of Advanced Industrial Science and Technology (AIST), 1-8-31 Midorigaoka, Ikeda, Osaka 563-8577, Japan

ABSTRACT: Controlling the molecular orientation of the conjugated oligomer, α-sexithiophene (6T), is crucial to improve organic optoelectronic device performance. Most 6T molecules evaporated onto quartz and SiO_2/Si substrates orient nearly perpendicular to the substrate. Here, we report the formation of oriented thin films of 6T on in-plane-oriented polythiophene (PT) films formed by the friction-transfer method. 6T was evaporated onto oriented PT films under vacuum. The films were investigated by polarized optical microscopy, polarized ultraviolet−visible light (UV−vis) absorption spectroscopy, and grazing incidence X-ray diffraction measurement (GIXD). In all spectra, larger absorbance derived from PT and 6T was observed, in parallel polarization to the friction direction, compared to that of orthogonal polarization. These results indicate that the 6T molecular axis is aligned in the friction direction (PT chain direction) of PT films. GIXD also confirmed that the 6T molecular axis was aligned parallel to the PT chain axis. In contrast, 6T molecules evaporated onto quartz and poly(ethylenedioxythiophene):poly(styrenesulfonate) (PEDOT:PSS)-coated silicon substrates aligned nearly perpendicular to the substrate. These results indicate that oriented PT films induce 6T orientation parallel to the PT chain direction.

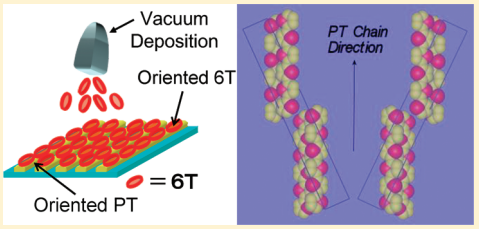

1. INTRODUCTION

The molecular orientation of conjugated polymers and/or oligomers significantly affects the performance of organic optoelectronic devices. For example, Sirringhaus et al. investigated field-effect transistors (FETs) consisting of poly(3-hexylthiophene) (P3HT), and clarified the relationship between charge transport properties and molecular orientation of the polymers, which involves the π−π stacking direction of thiophene rings.[1] DeLongchamp et al. investigated the anisotropic field-effect hole mobility of oligothiophenes, and showed that the mobility was over 10-fold higher when the oligothiophene molecules were standing on the substrate than when they were lying on the substrate.[2] This is because intermolecular π-electrons' overlap, such as herringbone or cofacial π-stacking, between oligothiophene molecules standing on the substrate leads to higher mobility in the direction parallel to the substrate, resulting in an increase in FET performance when bias voltage is applied between source and drain electrodes of the FET. On the other hand, for organic photovoltaic (OPV) devices, where bias voltage is applied between top and bottom electrodes, the increase in mobility in the direction perpendicular to the substrate will lead to improved power conversion efficiency. This could be achieved if oligothiophene molecules lie on the substrate, with π-electrons overlap, leading to an improvement of the mobility in the direction perpendicular to the substrate.[3,4] Moreover, incident light is absorbed much more efficiently by lying oligothiophenes than by standing ones.

The oligothiophene α-sexithiophene (6T) is a very promising material for application in organic electronic devices, such as thin film transistors,[5] thin film OPVs,[6] and organic light-emitting diodes (OLEDs).[7] When evaporated onto quartz and SiO_2/Si substrates, most 6T molecules tend to orient nearly perpendicular to the substrate. However, oriented thin films of 6T parallel to the substrate are required to improve the efficiency of the OPVs, as described above. In-plane 6T orientation was observed when the molecules were evaporated onto the native steps of a cleaved KBr(001)[8] and onto an ordered TiO_2(110)[9] substrates. However, these substrates are not suitable for OPV device application. Oriented thin films of 6T parallel to the substrate have been easily formed on oriented poly(tetrafluoroethylene) (PTFE) films prepared by the friction-transfer method;[10] however, PTFE is not a conductive polymer; i.e., it is also not suitable for OPV device application.

We have been using the friction-transfer method for the fabrication of oriented thin films of various conjugated polymers in which polymer backbones are aligned uniaxially.[11−15] Recently, we applied this method for the preparation of conductive polythiophene (PT) polymer thin films and observed excellent orientation of the PT molecules parallel to quartz and SiO_2/Si substrates.[16] We also found that vacuum-deposited oligomers were uniaxially aligned along the friction-transferred chains of conjugated polymers.[17,18]

Here, we report the formation of oriented thin films of 6T on oriented PT films. Because the constituent unit of 6T is the same as that of PT, and 6T and PT have similar crystalline structures, one can expect 6T films to grow epitaxially on friction-transferred PT films. Orientation of the 6T films was determined by polarized optical microscopy, polarized ultraviolet−visible light

Received: August 5, 2011
Revised: December 7, 2011
Published: December 09, 2011

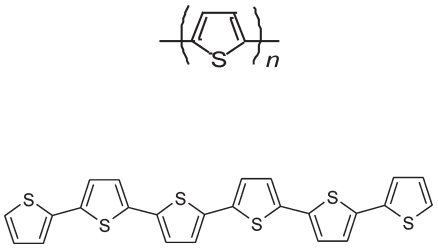

Figure 1. Chemical structures of PT (a, upper) and 6T (b, lower).

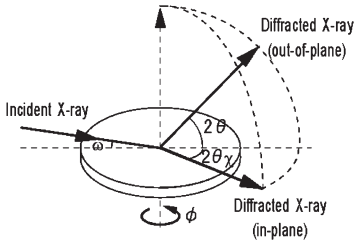

Figure 2. Geometry of GIXD measurements.

(UV−vis) absorption spectroscopy, and grazing incidence X-ray diffraction measurement (GIXD).

2. EXPERIMENTAL SECTION

PT and 6T were purchased from Aldrich Chemical Co., Inc., and Tokyo Chemical Industry Co., Ltd., respectively, and used without further purification. The chemical structures of PT and 6T are shown in Figure 1.

The PT powder was compressed into a pellet under vacuum. The friction transfer process was carried out by squeezing and drawing this PT pellet on quartz and Si substrates, heated at 250 °C. The applied load for squeezing was 20 kgf/cm^2, and the drawing speed was 1 m/min. The PT thickness was about 5 nm and roughness was less than 4 nm.

6T films between 5.0 and 50.0 nm in thickness were deposited onto the PT films under vacuum. The 6T deposition rates were 1.0−1.5 nm/min for the 5.0 nm thick film and 2.5−3.0 nm/min for the 25.0−50.0 nm thick ones.

For comparison analysis, 6T was also evaporated directly onto the substrates.

Polarized optical microscopy was carried out using an Olympus BX 51 with a polarizing filter. Quartz was used as the substrate for the films analyzed by optical microscopy.

UV−vis absorption spectra were measured using a Shimadzu UV-3150 spectrophotometer with a Glan−Taylor polarizing prism at an angle of incidence of 0°. Quartz was used as the substrate for the films analyzed by UV−vis spectroscopy.

The GIXD measurements were performed at BL46XU beamlines of SPring-8 (Japan Synchrotron Radiation Research Institute (JASRI)) equipped with ATX-GSOR (Rigaku Co.). The wavelength, λ, of monochromatized incident X-ray was 0.118 nm and the beam size was 0.5 mm × 0.1 mm. The grazing angle of incident X-ray, ω, was fixed at 0.14° to ensure total reflection from the silicon substrate. The GIXD profiles are represented in reciprocal space with scattering vector ($Q = 4\pi \sin\theta/\lambda$, where θ and λ are the Bragg angle and the wavelength of the incident X-rays, respectively). The out-of-plane X-ray scattering vector Q_z and the in-plane X-ray scattering vector Q_{xy} were positioned perpendicular and parallel to the film surface, respectively (Figure 2). The angle, χ, between the in-plane scattering vector and the drawing direction of friction-transfer was fixed during the in-plane $\phi - 2\theta\chi$ scan. For the out-of-plane 2θ scan and the in-plane $\phi - 2\theta\chi$ scan, the scan speeds were 10°/min and 20°/min, respectively, and the angular interval between steps was 0.02°. The molecular orientation distribution was determined by the rocking-curve scan. Changes in scattered intensity with sample rotation ϕ at a locked Q corresponded to the distribution of orientation of the diffracted lattice plane. For rocking-curve scan, the scan speed was 20°/min, and angular interval between steps was 0.1°. The sample was placed into a special holder covered with a Kapton hemisphere dome 200 mm in diameter and purged with helium gas during GIXD measurement. This replacement of air with helium gas was performed to reduce the background intensity and to prevent sample oxidation.

Silicon wafers were used as substrates for the GIXD measurements. Poly(ethylenedioxythiophene):poly(styrenesulfonate) (PEDOT:PSS; Aldrich Chemical Co., Inc.) was spin-coated onto the silicon substrate to improve PT film deposition reproducibility (thickness, orientation, etc.). 50.0 nm thick 6T films (deposition rate 2.5−3.0 nm/min) were deposited on both the PT/PEDOT:PSS/Si and PEDOT:PSS/Si substrates for comparison studies.

3. RESULTS AND DISCUSSION

3.1. Polarized Optical Microscopy. Figure 3, a and b, shows optical microscopic images (cross polarized) of a 25.0 nm thick 6T film deposited on the PT film, produced by the friction-transfer method, and on a quartz substrate, respectively. Numerous streaks or steps, originating from the oriented PT film, can be seen extending over the whole film in the friction direction (from lower left to upper right in Figure 3a). All areas of the 6T-deposited friction-transferred PT film changed alternately between bright and dark for every 45° rotation. Bright and dark contrast of the PT without the 6T film on top was much lower (data not shown). These results indicate that 6T molecules are aligned parallel to the PT chain direction through most of the film. In contrast, the 6T-deposited quartz substrate did not show birefringence. These observations indicate that 6T molecules might be uniaxially oriented perpendicular to the substrate or randomly oriented on the substrate.

3.2. Polarized UV−Vis Absorption Spectroscopy. Figure 4 shows the polarized UV−vis spectra of 6T-deposited friction-transferred PT films (Figure 4a,b), a friction-transferred PT film (Figure 4c), and a 6T film (Figure 4d) on a quartz substrate for optical polarization parallel (solid) and orthogonal (dashed) to the friction direction. In Figure 4, a and b, one can see that the absorbance derived from both the PT and 6T, around 550 and 380 nm, respectively, in parallel polarization was larger than that derived from orthogonal polarization, for all spectra.

The polarized UV−vis spectra of 6T from 6T-deposited PT films were determined by subtracting the spectrum of the PT film from the spectra of 6T-deposited PT films (data not shown).

The dichroic ratio, D_{abs}, is defined by eq 1

$$D_{abs} = A_{para}/A_{orth} \quad (1)$$

where A_{para} and A_{orth} are integrated absorbance in the range between 300 and 800 nm of the parallel and orthogonal polarized UV−vis spectra, respectively. D_{abs} gives information about the anisotropy of the absorption process. The electron transition

dx.doi.org/10.1021/jp207487z |J. Phys. Chem. B 2012, 116, 189–193

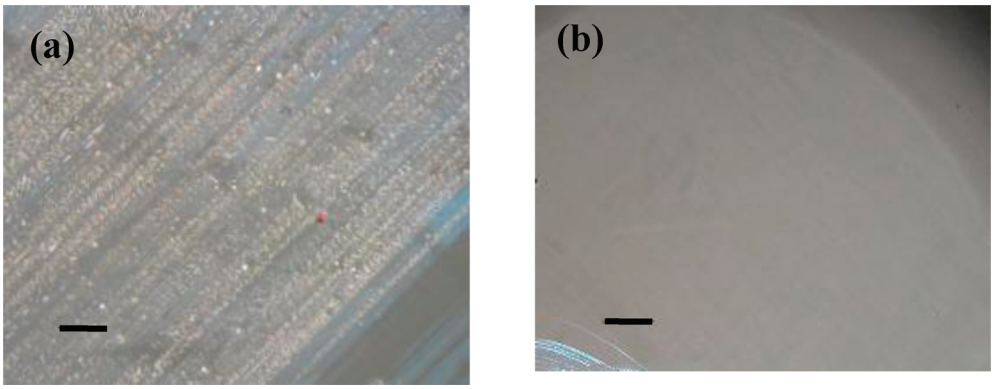

Figure 3. Optical photomicrographs under the Cross−Nicol condition of a 25 nm thick vapor-deposited 6T film on the PT film formed by the friction-transferred method (a) and a 25 nm thick vapor-deposited 6T film on the quartz substrate (b) (scale bar = 100 nm). Sliding direction of the PT pellet in panel (a) is from lower left to upper right.

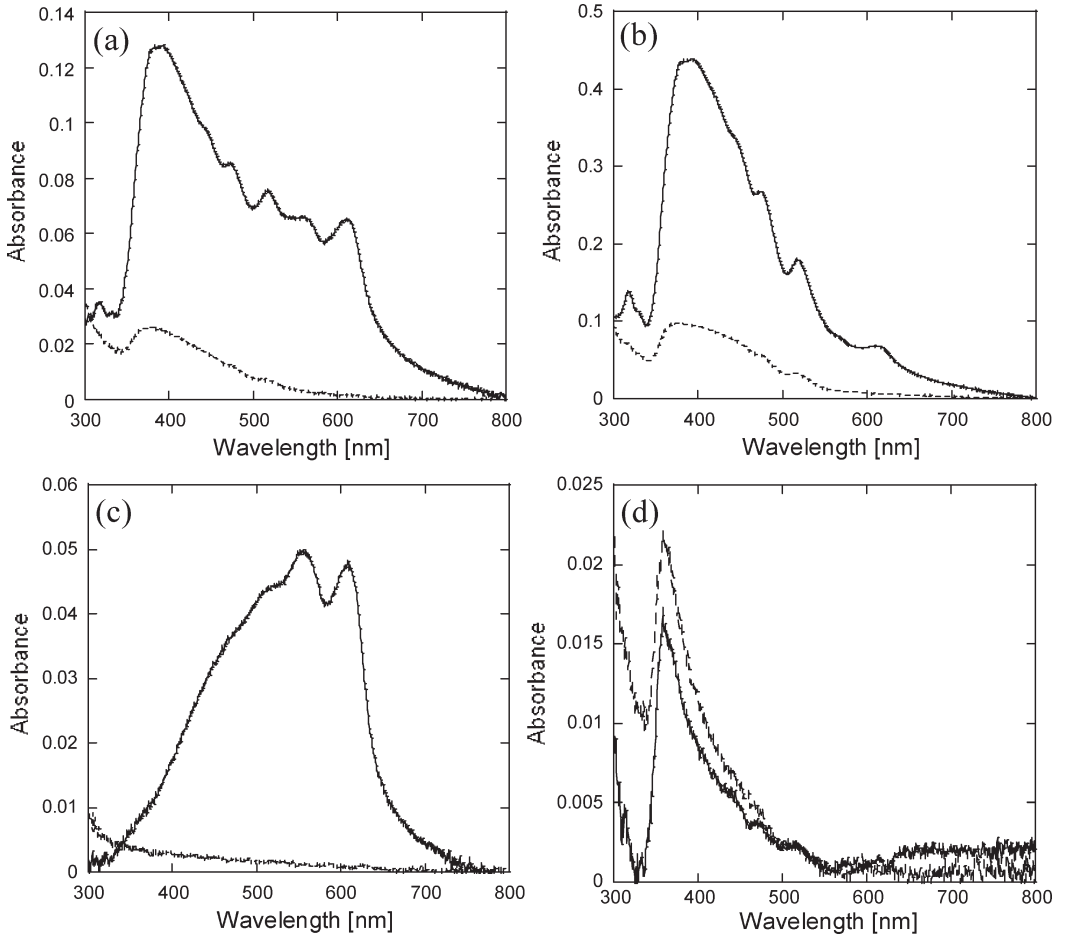

Figure 4. Polarized UV−vis spectra of 6T-deposited PT film formed by the friction-transfer method with thicknesses of (a) 5 nm and (b) 25 nm. Spectra measured with light parallel (solid line) and orthogonal (dotted line) to the friction direction. (c) Polarized UV−vis spectra of PT film formed by the friction-transfer method. (d) Polarized UV−vis spectra of 6T film with a thickness of 8 nm formed by vacuum deposition on a quartz substrate.

probability is maximized when the transition moment of the molecule lies parallel to the electric vector of the light.[19]

D_{abs} values of the 6T-deposited PT film with 6T thicknesses of 5.0 and 25.0 nm were 5.49 and 4.22, respectively. (Note that the PT film showed no absorption with orthogonal polarization.) This result indicates that the 6T molecular axis is aligned in the friction direction in the friction-transferred PT films. In addition, D_{abs} decreased as the thickness of 6T film increased, probably due to increase of in-plane molecular disorder of the 6T with increasing film thickness.

On the other hand, the 6T film deposited on the quartz substrate had no structural anisotropy, as can be seen in Figure 4d, which shows that the 6T molecular axis is not aligned in the plane of the substrate. In addition, the absorbance of 6T deposited on quartz was much lower than that of 6T deposited

dx.doi.org/10.1021/jp207487z |*J. Phys. Chem. B* 2012, 116, 189–193

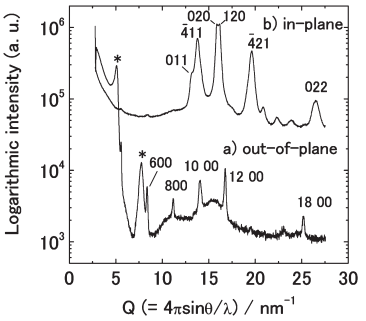

Figure 5. GIXD profiles of 6T/PEDOT:PSS/Si-wafer.

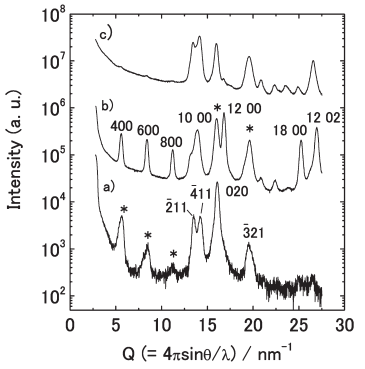

Figure 6. GIXD profiles of 6T/friction-transferred PT/PEDOT:PSS/Si-wafer: (a) out-of-plane; (b) in-plane with $\phi = 25°$; (c) in-plane with $\phi = 0°$.

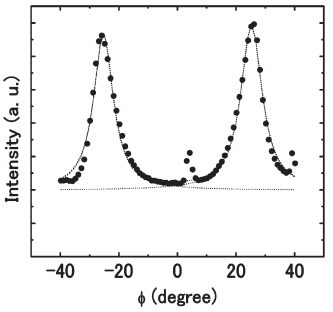

Figure 7. Rocking curve for 600 reflection ($Q = 8.25$ nm^{-1}).

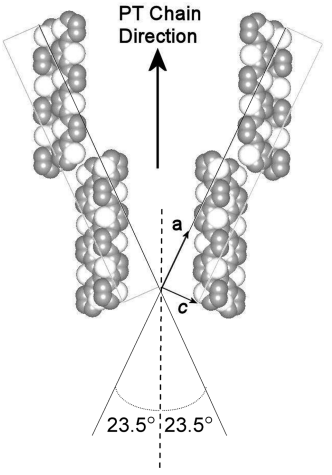

Figure 8. Molecular model of 6T depicting the twinned orientations of the unit cell.

on the friction-transferred PT. Hotta et al. reported that, in oligomer molecules with a well-defined molecular long axis, the transition dipole moment is nearly parallel to that axis.[20] In the films with vertical alignment, the direction of the transition dipole moment of the molecules was orthogonal to the direction of the oscillating electric vector of the incident light at an incident angle of 0° (perpendicular to the substrate), resulting in a marked decrease in the absorbance of the molecules. Therefore, one can say that 6T molecules deposited on a quartz substrate are probably aligned nearly perpendicular to the substrate.

3.3. Grazing Incidence X-ray Diffraction Measurement (GIXD). We carried out GIXD measurements to determine the detailed orientational structure of the 6T films. First, we present the results for 6T/PEDOT:PSS/Si, i.e., 6T film prepared without friction-transferred PT (Figure 5). Generally, 6T molecules tend to stand on substrates with an amorphous surface.[21] We observed obvious differences between GIXD profiles measured with in-plane and out-of-plane geometries, suggesting that 6T crystallites have some preferential orientation perpendicular to the substrate as discussed in the following. Almost all of the observed reflections can be indexed with the monoclinic unit cell, $a = 4.4708$ nm, $b = 0.7851$ nm, $c = 0.6029$ nm, and $\beta = 90.76°$, as reported by Horowitz.[22] The reflections indicated with asterisks in Figure 5a cannot be indexed by the unit cell, and they should be attributed to another crystal phase, which has been reported previously.[21,23] The $h00$ reflections, 600, 800, 1000, 1200, and 1800, can be seen in the out-of-plane diffraction, in which the scattering vector is normal to the substrate (Figure 5a). On the other hand, the $0kl$ reflections, 011, 020, and 022, appear in the in-plane diffraction, in which the scattering vector is parallel to the substrate (Figure 5b). These results suggest that the a-axis is almost normal to the substrate plane. Furthermore, relatively strong reflections $\bar{4}11$ (with $\bar{3}11$ and $\bar{2}11$) and $\bar{4}21$ (with $\bar{3}21$ and $\bar{2}21$) appear in the in-plane direction (Figure 5b). These reflections correspond to the distances of adjacent molecules, which stacking axis is parallel to the substrate.

On the other hand, there were large differences in diffraction profile for the 6T on the friction-transferred PT film (Figure 6). $\bar{2}11$, $\bar{4}11$, 020, and $\bar{3}21$ reflections were observed with $h00$ reflections, which are indicated by asterisks, in the out-of-plane diffraction (Figure 6a). In this measurement, some peripheral regions that are only covered by 6T (without PT underneath) were also exposed because, at glancing incident angle, the X-ray beam spreads over these regions. We considered the $h00$ reflections to originate from these peripheral areas of 6T without PT underneath. We observed a sharp and strong series of $h00$ reflections with the in-plane measurements. However, the diffraction intensity of these reflections was strongly dependent on the sample rotation (ϕ) in the substrate plane because the 6T crystallites were highly oriented in-plane. We rotated the sample around the angle ϕ to maximize the $h00$ reflections. The angle $\phi = 0$ is defined as the angle where the X-rays are irradiated parallel to the friction direction of the PT film. The $h00$ reflections were strongly observed at a rotation angle $\phi = 25°$. The $h00$ reflections, 400, 600, 800, 1000, and 1800 can be seen in Figure 6b. (Note that asterisks in Figure 6b indicate the 020 and $\bar{3}21$ reflections which probably originate from the peripheral areas of 6T without PT underneath, as described above.) These $h00$ reflections disappeared when the sample was further rotated (e.g., $\phi = 0°$ in Figure 6c). Changes in the scattered intensity at a locked Q, depending on

dx.doi.org/10.1021/jp207487z |J. Phys. Chem. B 2012, 116, 189–193

the sample rotation ϕ, correspond to the distribution of the local orientation of the crystal lattice. Figure 7 shows the rocking curve of the 600 diffraction plane at a fixed $Q = 8.25\ nm^{-1}$, measured with the sample rotation in ϕ between −40 and +40°. The rocking curves of the 600 diffraction plane showed a set of the two distributions with symmetrical centers at ca. ±25° and with similar half-width of distribution, i.e., 8.4°, suggesting that two types of arrangements of 6T crystals are present. This result can be explained considering the model in which the 6T molecular long axis and the *a*-axis (or the *a**-axis within less than 1°) make an angle of 23.5° in the unit cell.[22] If we assume that the 6T molecular long axis is aligned parallel to the PT chain axis (i.e., the friction direction), we have to consider that two types of crystals arrangement are equivalent, i.e., with the 6T cell's *a*-axis rotated about +23.5° and −23.5° from the friction direction (see Figure 8). This crystal arrangement was reported by Wittmann et al.,[24] for 6T-deposited friction-transferred PTFE films after electron diffraction measurements. We emphasize that not the crystal axis but the molecular axis of 6T is highly oriented parallel to the PT chain axis. The half-width of the distribution, 8.4°, is twice the orientational distribution of the friction-transferred PT, 4.1°.[16] These observations indicate that a friction-transferred PT film induces 6T crystallites to orient on top of these PT films, with molecular axis parallel to the PT molecular (friction) direction.

4. CONCLUSIONS

Here, we reported the formation of 6T films with the 6T molecules oriented parallel to the substrates on in-plane oriented PT films formed by the friction-transfer method. Analyses were performed by polarized optical microscopy, polarized UV−vis absorption spectroscopy, and GIXD. Polarized optical microscopy showed that 6T molecules were aligned parallel to the PT chain direction through most of the film. The results of polarized UV−vis absorption spectroscopy indicated that the 6T molecular axis was aligned parallel to the PT chain direction, and that in-plane molecular disorder of the 6T increased with increasing thickness of 6T film. In contrast, 6T molecules deposited on quartz were aligned nearly perpendicular to the substrate.

By GIXD measurements, we succeeded in evaluating the orientation distribution quantitatively, which was difficult using electron diffraction measurements reported previously.[24] GIXD measurements indicated that 6T molecules were highly oriented in the 6T films, showing that oriented PT films formed by the friction-transfer method strongly induced 6T orientation, parallel to the orientation of the PT films.

The 6T films grew epitaxially on the friction-transferred PT films. Possible reasons for the epitaxial nucleation and film growth mechanism are (1) chemical interaction[25] between 6T and the PT crystals and (2) kinetic mediated by the substrate surface morphology[8,9] derived from the oriented PT chains.

Considering that the constituent unit of 6T is the same as that of PT, and 6T and PT have similar crystalline structures, we suggest that the oriented crystals of 6T grow epitaxially on friction-transferred PT films mostly due to the chemical interaction.

The high hole mobility is in the direction orthogonal to the molecular long axis of crystalline films of 6T. Therefore, devices produced with oriented 6T films parallel to conductive PT substrates are expected to show increased current density through the films, resulting in improved performance of OPVs and OLEDs. Devices based on 6T films grown on friction-transferred PT films are currently prepared in our lab.

AUTHOR INFORMATION

Corresponding Author

*E-mail: chem42@ni.aist.go.jp. Tel: +81-72-751-7884. Fax: +81-72-751-9637.

ACKNOWLEDGMENT

We thank Dr. T. Koganesawa (JASRI), Dr. Y. Yoshida (AIST), Dr. N. Oohashi (AIST), and Dr. Y. Kojima (Mitsubishi Chemical Co., Inc.) for help with the GIXD measurements. We also thank Dr. Tracy Allgood (Cambridge Crystallographic Data Centre) for providing the 6T crystal structure data in electronic CIF format.

REFERENCES

(1) Sirringhaus, H.; Brown, P. J.; Friend, R. H.; Nielsen, M. M.; Bechgaard, K.; Langeveld-Voss, B. M. W.; Spiering, A. J. H.; Janssen, R. A. J.; Meijer, E. W.; Herwig, P.; de Leeuw, D. M. *Nature* **1999**, *401*, 685–688.

(2) DeLongchamp, D. M.; Jung, Y. S.; Fischer, D. A.; Lin, E. K.; Chang, P.; Subramanian, V.; Murphy, A. R.; Frechet, J. M. J. *J. Phys. Chem. B* **2006**, *110*, 10645–10650.

(3) Videlot, C.; Fichou, D. *Synth. Met.* **1999**, *102*, 885–888.

(4) Videlot, C.; Kassmi, A.; El; Fichou, D. *Sol. Energy Mater. Sol. Cells* **2000**, *63*, 69–82.

(5) Sandberg, H.; Henze, O.; Sirringhaus, H.; Kilbinger, A. F. M.; Feast, W. J.; Friend, R. *Proc. SPIE* **2001**, *4466*, 35–43.

(6) Sakai, J.; Taima, T.; Saito, K. *Org. Electron.* **2008**, *9*, 582–590.

(7) Heck, C.; Mizokuro, T.; Misaki, M.; Azumi, R.; Tanigaki, N. *Jpn. J. Appl. Phys.* **2011**, *50*, 04DK20.

(8) Ikeda, S.; Kiguchi, M.; Yoshida, Y.; Yase, K.; Mitsunaga, T.; Inaba, K.; Saiki, K. *J. Cryst. Growth* **2004**, *265*, 296–301.

(9) Ivanco, J.; Haber, T.; Krenn, J. R.; Netzer, F. P.; Resel, R.; Ramsey, M. G. *Surf. Sci.* **2007**, *601*, 178–187.

(10) Lang, P.; Horowitz, G.; Valat, P.; Garnier, F.; Wittmann, J. C.; Lotz, B. *J. Phys. Chem. B* **1997**, *101*, 8204.

(11) Tanigaki, N.; Yase, K.; Kaito, A.; Ueno, K. *Polymer* **1995**, *36*, 2477–2480.

(12) Tanigaki, N.; Yase, K.; Kaito, A. *Mol. Cryst. Liq. Cryst.* **1995**, *267*, 335–340.

(13) Tanigaki, N.; Kyotani, H.; Wada, M.; Kaito, A.; Yoshida, Y.; Han, E. M.; Abe, K.; Yase, K. *Thin Solid Films* **1998**, *331*, 229–238.

(14) Nagamatsu, S.; Takashima, W.; Kaneto, K.; Yoshida, Y.; Tanigaki, N.; Yase, K.; Omote, K. *Macromolecules* **2003**, *36*, 5252–5257.

(15) Misaki, M.; Ueda, Y.; Nagamatsu, S.; Yoshida, Y.; Tanigaki, N.; Yase, K. *Macromolecules* **2004**, *37*, 6926–6931.

(16) Takechi, C.; Tanigaki, N.; Nagamatsu, S.; Yoshida, Y. To be submitted for publication.

(17) Yoshida, Y.; Tanigaki, N.; Yase, K.; Hotta, S. *Adv. Mater.* **2000**, *12*, 1587–1591.

(18) Yase, K.; Han, E. M.; Yamamoto, K.; Yoshida, Y.; Takada, N.; Tanigaki, N. *Jpn. J. Appl. Phys.* **1997**, *36*, 2843–2848.

(19) Nagamatsu, S.; Misaki, M.; Chikamatsu, M.; Kimura, T.; Yoshida, Y.; Azumi, R.; Tanigaki, N.; Yase, K. *J. Phys. Chem. B* **2007**, *111*, 4349–4354.

(20) Hotta, S.; Ichino, Y.; Yoshida, Y.; Yoshida, M. *J. Phys. Chem. B* **2000**, *104*, 10316–10320.

(21) Lovinger, A. J.; Davis, D. D.; Ruel, R.; Torsi, L.; Dodabalapur, A.; Katz, H. E. *J. Mater. Res.* **1995**, *10*, 2958–2962.

(22) Horowitz, G.; Bachet, B.; Yassar, A.; Lang, P.; Demanze, F.; Fave, J. L.; Garnier, F. *Chem. Mater.* **1995**, *7*, 1337–1341.

(23) Servet, B.; Horowitz, G.; Ries, S.; Lagorsse, O.; Alnot, P.; Yassar, A.; Deloffre, F.; Srivastava, P.; Hajlaoui, R.; Lang, P.; Gamier, F. *Chem. Mater.* **1994**, *6*, 1809–1815.

(24) Wittmann, J. C.; Straupe, C.; Meyer, S.; Lotz, B.; Lang, P.; Horowitz, G.; Garnier, F. *Thin Solid Films* **1997**, *303*, 207.

(25) Ueda, Y.; Matsushita, M.; Morimoto, S.; Ni, J. P.; Suzuki, H.; Mashiko, S. *Thin Solid Films* **1998**, *331*, 216–221.